Precision Joint Constraints on Cosmology and Gravity Using Strongly Lensed Gravitational Wave Populations

Xinguang Ying[1] and Tao Yang [ID][1, *]

[1]*School of Physics and Technology, Wuhan University, Wuhan 430072, China*
(Dated: May 15, 2025)

We present a unified Bayesian framework to jointly constrain the Hubble constant H_0 and the post-Newtonian parameter γ, a key probe of deviations from general relativity, using the population characteristics of strongly lensed gravitational wave (GW) events from binary black hole mergers. Unlike traditional methods that rely on electromagnetic counterparts or GW waveform modeling, our approach exploits the time-delay distribution and the total number of lensed events, achievable with third-generation detectors such as the Einstein Telescope. Assuming a flat ΛCDM cosmology, we demonstrate that this method can achieve precision levels of $0.4\% - 0.7\%$ for H_0 and $0.5\% - 3.3\%$ for γ at 68% credibility, significantly outperforming existing joint constraints. These results underscore the power of lensed GW population statistics as a robust and efficient probe of both cosmic expansion and the nature of gravity.

I. INTRODUCTION

The first direct detection of gravitational waves (GWs) by LIGO/Virgo [1] marked the beginning of a new era in gravitational wave astronomy. Since the first observation of the binary black hole (BBH) merger event GW150914, an expanding catalog of gravitational wave (GW) events has been compiled [2–7], enabling a wide range of astrophysical and cosmological applications. Notably, GWs can act as "standard sirens", providing an independent method for measuring cosmological parameters [8–10], and offer a promising approach to addressing the Hubble tension – an inconsistency between low-redshift ($z \lesssim 2$) observations from type Ia supernovae [11] and high-redshift ($z \sim 1100$) measurements from the cosmic microwave background [12].

GW standard sirens face several limitations in constraining cosmological parameters, primarily due to uncertainties in luminosity distance estimates [13]. Moreover, their effectiveness relies on the accuracy of waveform templates and the precision of the matched-filtering technique, which must simultaneously infer more than ten waveform parameters. One proposed alternative is to use time delays from strongly lensed GWs in combination with the redshifts and images of their electromagnetic (EM) counterparts [14]. The significantly higher precision of time-delay measurements from lensed GWs, compared to those from lensed quasars, enables more accurate cosmological constraints. However, since the detection of EM counterparts typically requires a neutron star in the binary system, the predominantly observed BBH merger events [7] generally do not qualify. To address this limitation, a recent method has been proposed that avoids reliance on EM counterparts [15, 16], by leveraging population-level features of lensed GW catalogs, such as the distribution of time delays and the total number of lensed events.

The effectiveness of population-based approach relies on the detection of a large number of lensed GW events. The third generation GW detectors, such as the Einstein Telescope [17] and Cosmic Explorer [18], are expected to achieve significantly enhanced sensitivity and broader frequency coverage. These detectors will be capable of detecting GW signals from stellar mass BBHs at redshifts of up to $z \sim 100$ [19], recording millions of BBH events per year [20]. This unprecedented event rate provides a solid foundation for implementing population-based statistical analyses.

Beyond cosmology, gravitational lensing (GL) offers a unique opportunity to test the validity of general relativity (GR). The parameterized post-Newtonian (PPN) framework [21], particularly the parameter γ, quantifies deviations from GR. While precise constraints on γ have been obtained through solar system experiments – such as the Cassini mission [22] – constraints at galactic and cosmological scales remain relatively unexplored. Currently, most galaxy-scale constraints on γ depend on prior knowledge of cosmological parameters, as demonstrated in observations of lenses such as ESO 325-G004 [23], RXJ1121-1231, and B1608+656 [24]. Only a limited number of studies have jointly constrained the Hubble constant and the PPN parameter γ using lensed EM signals [25–27]. In contrast, lensed GWs offer significant advantages over traditional lensed EM sources such as quasars, including higher precision in time-delay measurements and a substantially higher detection rate. While quasars are typically confined to low redshifts (e.g., $z \sim 1$), GW lensing can probe a much broader redshift range, extending up to $z \sim 10$. These unique characteristics make lensed GWs a promising tool for jointly constraining cosmological parameters and testing gravity, reaching beyond the capabilities of current observational methods.

While unlensed gravitational waves can also provide valuable constraints on modified gravity (MG) [28–32], their sensitivity and accuracy are highly dependent on the precision of waveform modeling and parameter es-

---

* Corresponding author yangtao@whu.edu.cn

timation. In contrast, the population-based lensed GW approach does not rely on the waveform of the signals. Given the low uncertainties in both time-delay measurements and the count of lensed events, this method is expected to serve as a more powerful and efficient probe of gravity, offering lower statistical error and significantly reduced computational cost.

In this paper, we present, for the first time, a unified Bayesian framework to jointly constrain the Hubble constant and the PPN parameter γ using the population characteristics of strongly lensed gravitational wave events. By combining the time-delay distribution with the number of lensed events, we quantify the joint sensitivity to both the background cosmology and potential deviations from general relativity. Assuming a flat ΛCDM cosmology, we parametrize the Hubble constant as $H_0 = 100h$ kms^{-1}Mpc^{-1}. Our results show that, under various assumptions for the prior of Ω_m, the uncertainties in h and γ fall within the ranges of $0.4\% \sim 0.7\%$ and $0.5\% \sim 3.3\%$, respectively, at the 68% credible level – representing a significant improvement over existing joint constraints.

II. INCORPORATING γ IN GL

We focus on the gravity test on the lensing galaxy and model the MG effect via a simple constant parameter γ. Since this parametrization cannot be extended to the cosmological scales, the distance-redshift relation won't change.

The time delay between lensed images A and B is given by

$$\Delta t_{AB} = (1 + z_l) \frac{D_s D_l}{c D_{ls}} \left[\phi(\theta_A, \beta) - \phi(\theta_B, \beta) \right], \quad (1)$$

where z_l is the redshift of lens, $\phi(\theta, \beta) = (\theta - \beta)^2/2 - \psi(\theta)$ is called the Fermat potential, and D_s, D_l and D_{ls} are the angular diameter distances from the earth to the source, from the earth to the lens and from the lens to the source respectively. For the singular isothermal sphere model, the lensing potential is $\psi(\theta) = \theta_E |\theta|$, where θ_E is the angular Einstein radius. The images' positions $\theta_{A,B}$ are solved from the lensing equation $\beta = \theta - \alpha(\theta)$ [33]. The deflection angle $\alpha(\theta)$ is obtained by taking the gradient of the lensing potential: $\alpha(\theta) = -\nabla \psi(\theta) = \text{sgn}(\theta) \theta_E$.

After introducing the PPN correction, the lensing potential becomes $\psi^{\text{PPN}} = \frac{1+\gamma}{2} \psi^{\text{GR}}$, and consequently, the deflection angle is modified to $\alpha^{\text{PPN}} = \frac{1+\gamma}{2} \alpha^{\text{GR}}$. From the lensing equation, the image positions can be solved as $\theta_\pm = \beta \pm \theta_E^{\text{PPN}}$, where $\theta_E^{\text{PPN}} = \frac{1+\gamma}{2} \theta_E^{\text{GR}}$ [34]. Substituting these results into the time delay expression Eq. (1), one can find that the time delay in the PPN framework becomes $\Delta t^{\text{PPN}} = \frac{1+\gamma}{2} \Delta t^{\text{GR}}$. With the expression of Δt^{GR} in Ref. [35], the time delay with PPN correction is given

by

$$\Delta t^{\text{PPN}} = 32\pi^2 \frac{1+\gamma}{2} \frac{y}{c} \left(\frac{\sigma}{c}\right)^4 (1 + z_l) \frac{D_{ls} D_l}{D_s}, \quad (2)$$

where y is the impact parameter, σ is the lens velocity dispersion and z_s is the redshift of source.

We model the lens as a SIS with a modified Schechter function [36]. The differential optical depth in GR is given by [37]

$$\frac{\partial^2 \tau}{\partial z_l \partial \sigma} = \frac{\partial n}{\partial \sigma}(z_l, \sigma) s_{cr}(z_l, \sigma) c \frac{dt}{dz_l}(z_l), \quad (3)$$

where the modified Schechter function is

$$\frac{\partial n}{\partial \sigma}(z_l, \sigma) = \frac{n_*}{\sigma_*} \frac{\beta}{\Gamma(\alpha/\beta)} \left(\frac{\sigma}{\sigma_*}\right)^{\alpha-1} \exp\left[-\left(\frac{\sigma}{\sigma_*}\right)^\beta\right]. \quad (4)$$

The cross section s_{cr} in GR is given by Ref. [37]. After introducing PPN correction, it becomes

$$s_{cr}^{\text{PPN}} = \pi D_l^2 \left(\theta_E^{\text{PPN}}\right)^2 \left[y_{\max}^2 - \frac{2\Delta t^{\text{PPN}}}{3 T_{\text{obs}} y} y_{\max}^3\right], \quad (5)$$

where the $y_{\max}$ is the maximum impact parameter and the T_{obs} is the observation duration. Integrating Eq. (3) generates the optical depth with PPN correction:

$$\tau(z_s, \mathbf{\Omega}) = \left(\frac{1+\gamma}{2}\right)^2 \frac{F_*}{30} \left[(1 + z_s) D_s\right]^3 y_{\max}^2$$
$$\times \left[1 - \frac{1+\gamma}{2} \frac{\Delta t_*}{7 T_{\text{obs}}} \frac{\Gamma\left[(8+\alpha)/\beta\right]}{\Gamma\left[(4+\alpha)/\beta\right]}\right], \quad (6)$$

where

$$F_* = 16\pi^3 n_* \frac{\sigma_*^4}{c^4} \frac{\Gamma\left[(4+\alpha)/\beta\right]}{\Gamma(\alpha/\beta)}, \quad (7)$$

$$\Delta t_* = 32\pi^2 \frac{\sigma_*^4}{c^4} \frac{D_s}{c} (1 + z_s) y_{\max}. \quad (8)$$

Here the parameters $\{n_*, \alpha, \beta, \sigma_*\}$, called the velocity dispersion function (VDF) parameters, have been extensively measured through observations of diverse galaxy populations [36, 38–41].

III. POPULATION METHOD

Assuming N lensed events have been detected with exact time delays $\{\Delta t_i\}_{i=1}^N$ between each lensed binary image signals during the observation period T_{obs}, the population characteristics of lensed GWs can be determined by two independent likelihoods given by N and $\{\Delta t_i\}$ respectively [15]:

$$\mathcal{L}\left(N, \{\Delta t_i\} | \mathbf{\Omega}, T_{\text{obs}}\right) = \mathcal{L}\left(N | \mathbf{\Omega}, T_{\text{obs}}\right) \times \mathcal{L}\left(\{\Delta t_i\} | \mathbf{\Omega}, T_{\text{obs}}\right), \quad (9)$$

where $\mathbf{\Omega} = (h, \Omega_m, \gamma)$.

Under the assumptions of event independence and negligible probability for multiple events occurring in a short interval, the likelihood of observing N lensed events is described by a Poisson distribution:

$$\mathcal{L}\left(N|\boldsymbol{\Omega}, T_{\text{obs}}\right) = \frac{\Lambda(\boldsymbol{\Omega}, T_{\text{obs}})^N e^{-\Lambda(\boldsymbol{\Omega}, T_{\text{obs}})}}{N!}. \qquad (10)$$

Here $\Lambda(\boldsymbol{\Omega}, T_{\text{obs}})$ is the expected number of lensed events over the observation duration T_{obs}, which can be expressed as [15]

$$\Lambda(\boldsymbol{\Omega}, T_{\text{obs}}) = R \int_0^{z_{\text{max}}} p_b(z_s|\boldsymbol{\Omega}) P_l(z_s|\boldsymbol{\Omega}) \mathrm{d}z_s \\ \times \int_0^{T_{\text{obs}}} p(\Delta t|\boldsymbol{\Omega})(T_{\text{obs}} - \Delta t)\mathrm{d}\Delta t, \quad (11)$$

where R denotes the BBH merger rate. The functions $p_b(z_s|\boldsymbol{\Omega})$, $P_l(z_s|\boldsymbol{\Omega})$ and $p(\Delta t|\boldsymbol{\Omega})$ are the redshift distribution of the merging binaries sources, the strong lensing probability, and the time delay distribution respectively. It's worth noting that the maximum source redshift z_{max} needs to be rescaled for different values of h and Ω_m, since the same detector sensitivity limit corresponds to the same maximum detectable luminosity distance.

Considering the independence among different events, the likelihood of observing the time delays $\{\Delta t_i\}$ is given by

$$p\left(\{\Delta t_i\}|\boldsymbol{\Omega}, T_{\text{obs}}\right) = \prod_{i=1}^N p(\Delta t_i|\boldsymbol{\Omega}, T_{\text{obs}}), \qquad (12)$$

where $p(\Delta t_i|\boldsymbol{\Omega}, T_{\text{obs}})$ is the value of the model time delay distribution $p(\Delta t|\boldsymbol{\Omega}, T_{\text{obs}})$ evaluated at Δt_i. The model time delay distribution is given by

$$p(\Delta t|\boldsymbol{\Omega}, T_{\text{obs}}) \propto p(\Delta t|\boldsymbol{\Omega})(T_{\text{obs}} - \Delta t)\Theta(T_{\text{obs}} - \Delta t). \quad (13)$$

To construct the redshift distribution of GW sources $p_b(z_s|\boldsymbol{\Omega})$, we assume the merger rate is uniform in comoving volume. The differential comoving volume at z_s is $\dot{V}_c(z_s) = 4\pi c(1 + z_s)^2 D_s^2/[H_0 E(z_s)]$. The observed merger rate includes a time dilation factor $(1 + z_s)^{-1}$, leading to $p_b(z_s|\boldsymbol{\Omega}) \propto \dot{V}_c(z_s)/(1 + z_s)$.

Considering the low proportion of lensed events among all GW events as suggested by current detections [42], the strong lensing probability can be approximated to be $P_l(z_s|\boldsymbol{\Omega}) = 1 - e^{-\tau(z_s, \boldsymbol{\Omega})} \approx \tau(z_s, \boldsymbol{\Omega})$, where $\tau(z_s, \boldsymbol{\Omega})$ is the strong lensing optical depth for an event originating from a source at redshift z_s.

The expected time delay distribution $p(\Delta t|\boldsymbol{\Omega})$ is generated by marginalizing the parameters $\boldsymbol{\lambda} = (y, \sigma, z_l, z_s)$, i.e.,

$$p(\Delta t|\boldsymbol{\Omega}) = \int p(\Delta t|\boldsymbol{\lambda}, \boldsymbol{\Omega}) p(\boldsymbol{\lambda}|\boldsymbol{\Omega}) \mathrm{d}\boldsymbol{\lambda}, \qquad (14)$$

where $p(\Delta t|\boldsymbol{\lambda}, \boldsymbol{\Omega})$ is the distribution of the time delay Δt given $\boldsymbol{\lambda}$ and $\boldsymbol{\Omega}$, and $p(\boldsymbol{\lambda}|\boldsymbol{\Omega})$ is the probability distribution

of the parameter vector $\boldsymbol{\lambda}$ given $\boldsymbol{\Omega}$. The latter can be split as

$$p(\boldsymbol{\lambda}|\boldsymbol{\Omega}) = p(\sigma, z_l|z_s, \boldsymbol{\Omega}) p_b(z_s|\boldsymbol{\Omega}) p(y|\boldsymbol{\Omega}), \qquad (15)$$

where $p(\sigma, z_l|z_s, \boldsymbol{\Omega}) \propto \partial^2\tau/\partial z_l\partial\sigma$. The distribution of lensed sources is assumed to be uniform within the Einstein radius on the lens plane, resulting in $p(y) \propto y$ for $y \in [0, 1]$.

IV. SIMULATIONS AND RESULTS

We assume the maximum of detectable redshift of the source under the "true" cosmology ($h = 0.7, \Omega_m = 0.3$) is $z_{\text{max}} = 20$. The lensing galaxy model is based on the VDF parameter measurements reported in Ref. [39]. The default merger rate and observation duration are $R = 5 \times 10^5\text{yr}^{-1}$ and $T_{\text{obs}} = 10\text{yrs}$ respectively.

To explore the dependence of the expected number of lensed events Λ on $\boldsymbol{\Omega}$, we present comparative plots in Fig. 1. We find that the same value of Λ can map to different combinations of (h, Ω_m, γ), indicating degeneracies among these parameters. Fig. 1 also illustrates that larger values of h and γ tend to increase the number of lensed events, while increasing Ω_m has the opposite effect. This trend can be understood as a consequence of the dependence of angular diameter distances on Ω_m, which results in a suppression of the lensing rate for larger Ω_m. This behavior is consistent with earlier findings reported in Ref. [43]. However, Ref. [15] reports an opposite trend, where higher Ω_m leads to more lensed events. This arises because Ω_m affects both cosmological distances and the lens population, with larger values resulting in more massive halos, thereby introducing additional sensitivity to Ω_m beyond geometric effects.

We then examine the influence of $\boldsymbol{\Omega}$ on the distribution of observed time delays $p(\Delta t|\boldsymbol{\Omega}, T_{\text{obs}})$. As shown in Fig. 2, variations of $\boldsymbol{\Omega}$ result in noticeable shifts in the shape and peak location of the time-delay probability density function (PDF). Specifically, increasing h or Ω_m shifts the peak of the distribution toward shorter time delays, while increasing γ moves the peak toward longer time delays. Besides, the overlap of different lines suggests the occurrence of degeneracy among h, Ω_m and γ. The concentration of time delays around several months aligns with expectations for galaxy-scale GL of GW [42, 44]. The shifting behavior with respect to Ω_m is qualitatively consistent with trends reported in Ref. [45, 46].

According to Bayes' theorem, the posterior is is proportional to the product of the likelihood Eq. (10) and the prior. We use Eqs. (11) and (13) to simulate the observed event number N and time delays $\{\Delta t_i\}$ respectively, assuming the true parameters $(h, \Omega_m, \gamma) = (0.7, 0.3, 1)$.

To check the validity of our model, we begin by constraining the cosmological parameters. Fig. 3 presents the joint constraints on h and Ω_m. Uniform priors over the following ranges are adopted: $0.6 < h < 0.8$, $0.2 <$
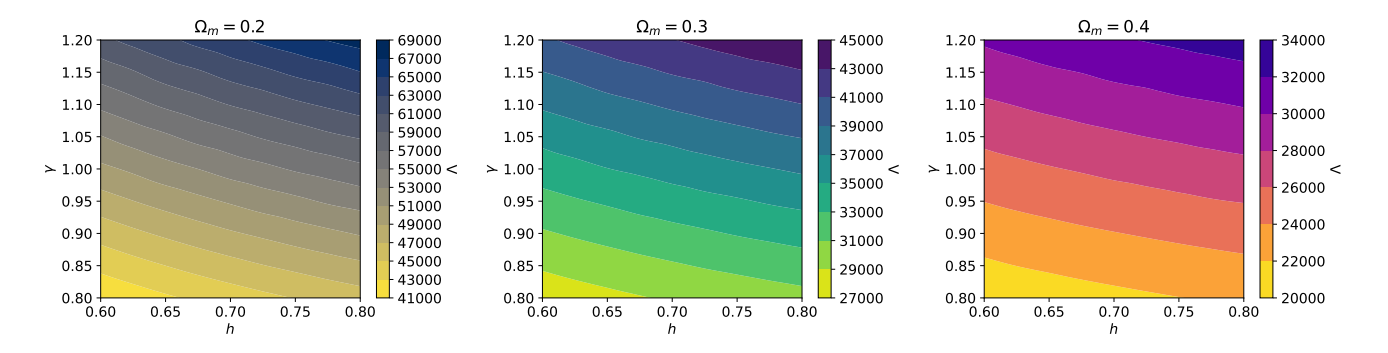
FIG. 1. Distributions of the lensed event number Λ in the $\gamma - h$ parameter space for three fixed values of Ω_m.

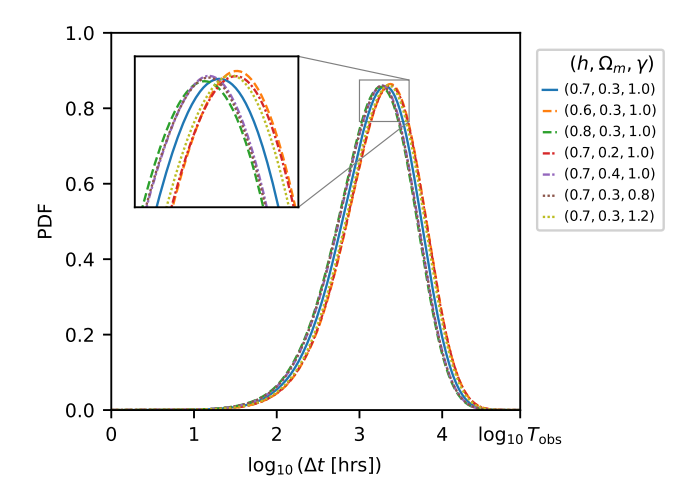FIG. 2. Observed PDF of the time delays with different values of $\mathbf{\Omega}$.

FIG. 3. Posterior distributions (68% and 95% credible regions) of h and Ω_m with γ fixed at 1. The 68% credible intervals yield the constraints: $h = 0.6999 \pm 0.0043$ and $\Omega_m = 0.3000 \pm 0.0015$.

$\Omega_m < 0.4$, with γ fixed at 1. The uncertainties are found to be 0.43% for h and 0.15% for Ω_m, which are comparable to those from other probes [11, 12], assuming GR holds.

We then consider two strategies to address the degeneracy among $\{h, \Omega_m, \gamma\}$ to simultaneously constrain h and γ. First, we fix the value of Ω_m at 0.3. Second, and more realistically, we model Ω_m as a Gaussian-distributed parameter with a standard deviation of $\sigma = 0.0056$, informed by Planck 2018 [12]. Uniform priors over the following ranges are adopted for both two strategies: $0.6 < h < 0.8$, $0.8 < \gamma < 1.2$. Fig. 4 shows the constraints obtained using the first strategy, while Fig. 5 presents the results from the second. As can be seen, the constraints on h and γ have uncertainties of $0.42\% \sim 0.69\%$ and $0.53\% \sim 3.3\%$, respectively, which are significantly more precise than the minimum uncertainties of 1.5% and 8.7% achieved by previous joint probes [25–27]. This demonstrates that the population-based statistics of lensed GW events holds great potential for joint constraints on cosmic expansion and gravity theories.
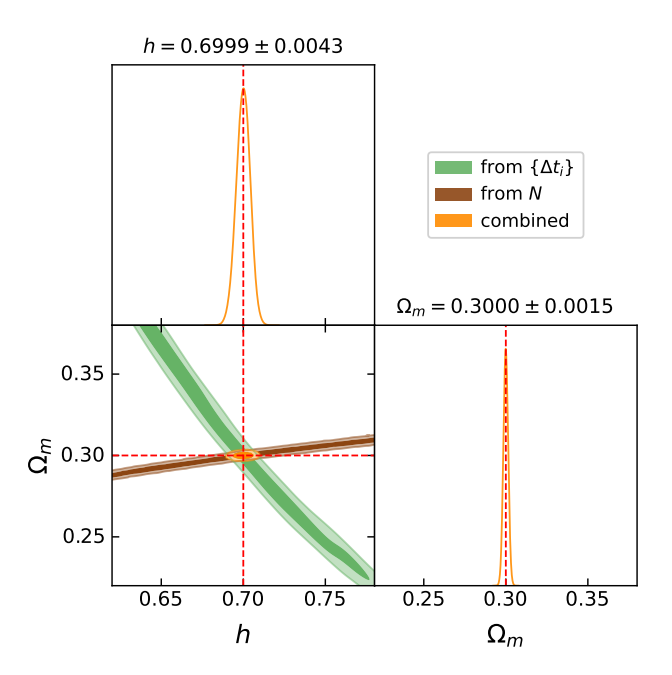
V. CONCLUSION AND DISCUSSION

We investigate the joint constraint of Hubble constant and post-Newtonian parameter γ from the population statistics of strongly lensed GWs originating from BBH mergers. The results demonstrate that this population-based approach offers significantly improved joint constraints relative to other existing joint probes. Notably, this method only depends on the observations of the time delay distribution and the total number of lensed GW events, no need the EM counterparts and GW waveform knowledge. Owing to the anticipated low uncertainties in both time delay measurements and event counts, this approach offers considerable potential for delivering power-
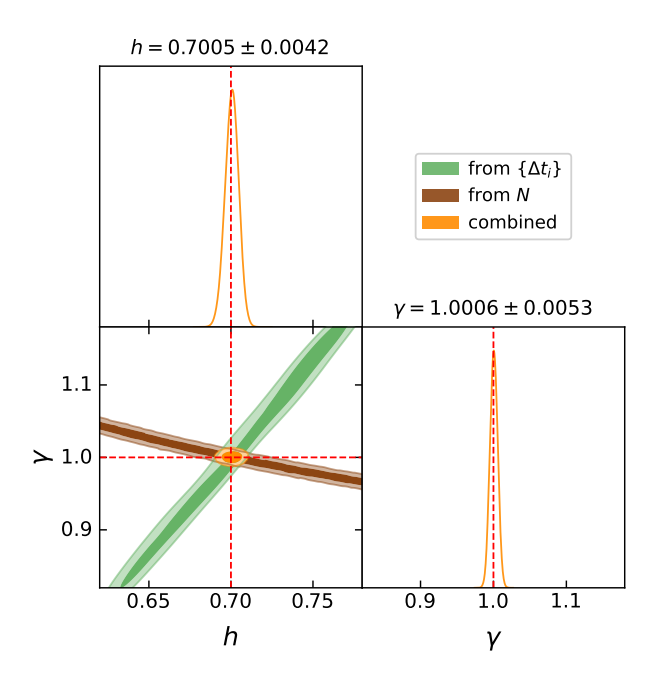
FIG. 4. Posterior distributions (68% and 95% credible regions) of h and γ with Ω_m fixed at 0.3. The 68% credible intervals yield the constraints: $h = 0.7005 \pm 0.0042$ and $\gamma = 1.0006 \pm 0.0053$.
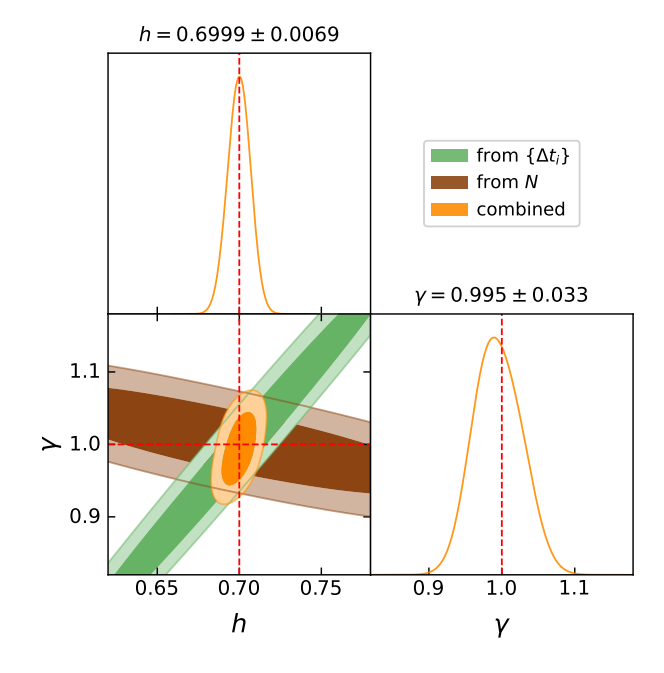

FIG. 5. Posterior distributions (68% and 95% credible regions) of h and γ with Ω_m assumed to follow a Gaussian distribution with the standard deviation $\sigma = 0.0056$. The 68% credible intervals yield the constraints: $h = 0.6999 \pm 0.0069$ and $\gamma = 0.995 \pm 0.033$.

ful and robust constraints, thereby serving as a promising joint probe for both cosmology and gravity.

There are several topics that can be explored in future work. Firstly, more source distribution models can be considered, such as those given by [47, 48]. In addition, more realistic lens models could be adopted, including the singular isothermal ellipsoid model [49], the generalized Navarro-Frenk-White model [50], and even the model based on numerically simulated dark matter halo mass function [51]. In such cases, it would be necessary to re-investigate how to properly incorporate the PPN parameter γ into these frameworks. Furthermore, extensions to other cosmological models (e.g., wCDM) and constraints on additional PPN parameters, are worth investigating. Lastly, a thorough analysis of systematic errors, such as uncertainties in the VDF parameters, should also be addressed. These aspects will be explored in detail in our future research.

[1] B. P. Abbott *et al.* (LIGO Scientific, Virgo), Observation of Gravitational Waves from a Binary Black Hole Merger, Phys. Rev. Lett. **116**, 061102 (2016), arXiv:1602.03837 [gr-qc].

[2] B. P. Abbott *et al.* (LIGO Scientific, Virgo), GWTC-1: A Gravitational-Wave Transient Catalog of Compact Binary Mergers Observed by LIGO and Virgo during the First and Second Observing Runs, Phys. Rev. X **9**, 031040 (2019), arXiv:1811.12907 [astro-ph.HE].

[3] B. Zackay, T. Venumadhav, L. Dai, J. Roulet, and M. Zaldarriaga, Highly spinning and aligned binary black hole merger in the Advanced LIGO first observing run, Phys. Rev. D **100**, 023007 (2019), arXiv:1902.10331 [astro-ph.HE].

[4] T. Venumadhav, B. Zackay, J. Roulet, L. Dai, and M. Zaldarriaga, New binary black hole mergers in the second observing run of Advanced LIGO and Advanced Virgo, Phys. Rev. D **101**, 083030 (2020), arXiv:1904.07214 [astro-ph.HE].

[5] A. H. Nitz, T. Dent, G. S. Davies, S. Kumar, C. D. Capano, I. Harry, S. Mozzon, L. Nuttall, A. Lundgren, and M. Tápai, 2-OGC: Open Gravitational-wave Catalog of binary mergers from analysis of public Advanced LIGO and Virgo data, Astrophys. J. **891**, 123 (2020), arXiv:1910.05331 [astro-ph.HE].

[6] R. Abbott *et al.* (LIGO Scientific, Virgo), GWTC-2: Compact Binary Coalescences Observed by LIGO and Virgo During the First Half of the Third Observing Run, Phys. Rev. X **11**, 021053 (2021), arXiv:2010.14527 [gr-qc].

[7] R. Abbott *et al.* (KAGRA, VIRGO, LIGO Scientific), GWTC-3: Compact Binary Coalescences Observed by LIGO and Virgo during the Second Part of the Third Observing Run, Phys. Rev. X **13**, 041039 (2023), arXiv:2111.03606 [gr-qc].

[8] B. F. Schutz, Determining the Hubble Constant from Gravitational Wave Observations, Nature **323**, 310 (1986).

[9] D. E. Holz and S. A. Hughes, Using gravitational-wave standard sirens, Astrophys. J. **629**, 15 (2005), arXiv:astro-ph/0504616.

[10] S. Nissanke, D. E. Holz, N. Dalal, S. A. Hughes, J. L. Sievers, and C. M. Hirata, Determining the Hubble constant from gravitational wave observations of merging compact binaries, (2013), arXiv:1307.2638 [astro-ph.CO].

[11] A. G. Riess *et al.*, A Comprehensive Measurement of the Local Value of the Hubble Constant with 1 km s^{-1} Mpc^{-1} Uncertainty from the Hubble Space Telescope and the SH0ES Team, Astrophys. J. Lett. **934**, L7 (2022), arXiv:2112.04510 [astro-ph.CO].

[12] N. Aghanim *et al.* (Planck), Planck 2018 results. VI. Cosmological parameters, Astron. Astrophys. **641**, A6 (2020), [Erratum: Astron.Astrophys. 652, C4 (2021)], arXiv:1807.06209 [astro-ph.CO].

[13] E. Chassande-Mottin, K. Leyde, S. Mastrogiovanni, and D. A. Steer, Gravitational wave observations, distance measurement uncertainties, and cosmology, Phys. Rev. D **100**, 083514 (2019), arXiv:1906.02670 [astro-ph.CO].

[14] K. Liao, X.-L. Fan, X.-H. Ding, M. Biesiada, and Z.-H. Zhu, Precision cosmology from future lensed gravitational wave and electromagnetic signals, Nature Commun. **8**, 1148 (2017), [Erratum: Nature Commun. 8, 2136 (2017)], arXiv:1703.04151 [astro-ph.CO].

[15] S. Jana, S. J. Kapadia, T. Venumadhav, and P. Ajith, Cosmography Using Strongly Lensed Gravitational Waves from Binary Black Holes, Phys. Rev. Lett. **130**, 261401 (2023), arXiv:2211.12212 [astro-ph.CO].

[16] S. Jana, S. J. Kapadia, T. Venumadhav, S. More, and P. Ajith, Strong-lensing cosmography using third-generation gravitational-wave detectors, Class. Quant. Grav. **41**, 245010 (2024), arXiv:2405.17805 [gr-qc].

[17] M. Punturo *et al.*, The Einstein Telescope: A third-generation gravitational wave observatory, Class. Quant. Grav. **27**, 194002 (2010).

[18] D. Reitze *et al.*, Cosmic Explorer: The U.S. Contribution to Gravitational-Wave Astronomy beyond LIGO, Bull. Am. Astron. Soc. **51**, 035 (2019), arXiv:1907.04833 [astro-ph.IM].

[19] E. D. Hall and M. Evans, Metrics for next-generation gravitational-wave detectors, Class. Quant. Grav. **36**, 225002 (2019), arXiv:1902.09485 [astro-ph.IM].

[20] M. Maggiore *et al.* (ET), Science Case for the Einstein Telescope, JCAP **03**, 050, arXiv:1912.02622 [astro-ph.CO].

[21] K. S. Thorne and C. M. Will, Theoretical Frameworks for Testing Relativistic Gravity. I. Foundations, Astrophys. J. **163**, 595 (1971).

[22] B. Bertotti, L. Iess, and P. Tortora, A test of general relativity using radio links with the Cassini spacecraft, Nature **425**, 374 (2003).

[23] T. E. Collett, L. J. Oldham, R. J. Smith, M. W. Auger, K. B. Westfall, D. Bacon, R. C. Nichol, K. L. Masters, K. Koyama, and R. van den Bosch, A precise extragalactic test of General Relativity, Science **360**, 1342 (2018), arXiv:1806.08300 [astro-ph.CO].

[24] D. Jyoti, J. B. Munoz, R. R. Caldwell, and M. Kamionkowski, Cosmic Time Slip: Testing Gravity on Supergalactic Scales with Strong-Lensing Time Delays, Phys. Rev. D **100**, 043031 (2019), arXiv:1906.06324 [astro-ph.CO].

[25] T. Yang, S. Birrer, and B. Hu, The first simultaneous measurement of Hubble constant and post-Newtonian parameter from Time-Delay Strong Lensing, Mon. Not. Roy. Astron. Soc. **497**, L56 (2020), arXiv:2003.03277 [astro-ph.CO].

[26] T. Liu and K. Liao, Determining cosmological-model-independent H0 and post-Newtonian parameter with time-delay lenses and supernovae, Mon. Not. Roy. Astron. Soc. **528**, 1354 (2024), arXiv:2309.13608 [astro-ph.CO].

[27] R. Gao, Z. Li, and H. Gao, Prospects of strongly lensed fast radio bursts: simultaneous measurement of post-Newtonian parameter and Hubble constant, Mon. Not. Roy. Astron. Soc. **516**, 1977 (2022), arXiv:2208.10175 [astro-ph.CO].

[28] B. P. Abbott *et al.* (LIGO Scientific, Virgo), Tests of General Relativity with the Binary Black Hole Signals from the LIGO-Virgo Catalog GWTC-1, Phys. Rev. D **100**, 104036 (2019), arXiv:1903.04467 [gr-qc].

[29] B. P. Abbott *et al.* (LIGO Scientific, Virgo), Tests of general relativity with GW150914, Phys. Rev. Lett. **116**,

221101 (2016), [Erratum: Phys.Rev.Lett. 121, 129902 (2018)], arXiv:1602.03841 [gr-qc].

[30] C. M. Will, The Confrontation between General Relativity and Experiment, Living Rev. Rel. **17**, 4 (2014), arXiv:1403.7377 [gr-qc].

[31] E. Belgacem, Y. Dirian, S. Foffa, and M. Maggiore, Gravitational-wave luminosity distance in modified gravity theories, Phys. Rev. D **97**, 104066 (2018), arXiv:1712.08108 [astro-ph.CO].

[32] T. Yang, Gravitational-Wave Detector Networks: Standard Sirens on Cosmology and Modified Gravity Theory, JCAP **05**, 044, arXiv:2103.01923 [astro-ph.CO].

[33] P. Schneider, J. Ehlers, and E. E. Falco, *Gravitational Lenses*, Astronomy and Astrophysics Library (Springer, 1992).

[34] A. S. Bolton, S. Rappaport, and S. Burles, Constraint on the Post-Newtonian Parameter gamma on Galactic Size Scales, Phys. Rev. D **74**, 061501 (2006), arXiv:astro-ph/0607657.

[35] M. Oguri, A. Taruya, Y. Suto, and E. L. Turner, Strong gravitational lensing time delay statistics and the density profile of dark halos, Astrophys. J. **568**, 488 (2002), arXiv:astro-ph/0112119.

[36] Y.-Y. Choi, C. Park, and M. S. Vogeley, Internal and Collective Properties of Galaxies in the Sloan Digital Sky Survey, Astrophys. J. **658**, 884 (2007), arXiv:astro-ph/0611607.

[37] M. Sereno, P. Jetzer, A. Sesana, and M. Volonteri, Cosmography with strong lensing of LISA gravitational wave sources, Mon. Not. Roy. Astron. Soc. **415**, 2773 (2011), arXiv:1104.1977 [astro-ph.CO].

[38] R. K. Sheth *et al.* (SDSS), The Velocity Dispersion Function of Early-Type Galaxies, Astrophys. J. **594**, 225 (2003), arXiv:astro-ph/0303092.

[39] A. D. Montero-Dorta, A. S. Bolton, and Y. Shu, A direct measurement of the high-mass end of the velocity dispersion function at $z \sim 0.55$ from sdss-iii/boss, Monthly Notices of the Royal Astronomical Society **468**, 47–58 (2017).

[40] K.-H. Chae, Galaxy evolution from strong lensing statistics: the differential evolution of the velocity dispersion function since z ~ 1, Mon. Not. Roy. Astron. Soc. **402**, 2031 (2010), arXiv:0811.0560 [astro-ph].

[41] J. L. Mitchell, C. R. Keeton, J. A. Frieman, and

R. K. Sheth, Robust cosmological constraints from gravitational lens statistics, Astrophys. J. **622**, 81 (2005), arXiv:astro-ph/0401138.

[42] R. Abbott *et al.* (LIGO Scientific, VIRGO), Search for Lensing Signatures in the Gravitational-Wave Observations from the First Half of LIGO–Virgo's Third Observing Run, Astrophys. J. **923**, 14 (2021), arXiv:2105.06384 [gr-qc].

[43] A. R. Cooray, An Upper limit on Omega(M) using lensed arcs, Astrophys. J. **524**, 504 (1999), arXiv:astro-ph/9904245.

[44] M. Oguri, Effect of gravitational lensing on the distribution of gravitational waves from distant binary black hole mergers, Mon. Not. Roy. Astron. Soc. **480**, 3842 (2018), arXiv:1807.02584 [astro-ph.CO].

[45] D. Harvey, A 4% measurement of H_0 using the cumulative distribution of strong-lensing time delays in doubly-imaged quasars, Mon. Not. Roy. Astron. Soc. **498**, 2871 (2020), arXiv:2011.09488 [astro-ph.CO].

[46] J.-J. Wei and X.-F. Wu, Strongly Lensed Gravitational Waves and Electromagnetic Signals as Powerful Cosmic Rulers, Mon. Not. Roy. Astron. Soc. **472**, 2906 (2017), arXiv:1707.04152 [astro-ph.CO].

[47] M. Dominik, K. Belczynski, C. Fryer, D. E. Holz, E. Berti, T. Bulik, I. Mandel, and R. O'Shaughnessy, Double Compact Objects II: Cosmological Merger Rates, Astrophys. J. **779**, 72 (2013), arXiv:1308.1546 [astro-ph.HE].

[48] K. Belczynski, D. E. Holz, T. Bulik, and R. O'Shaughnessy, The first gravitational-wave source from the isolated evolution of two 40-100 Msun stars, Nature **534**, 512 (2016), arXiv:1602.04531 [astro-ph.HE].

[49] R. Kormann, P. Schneider, and M. Bartelmann, Isothermal elliptical gravitational lens models, Astronomy and Astrophysics (ISSN 0004-6361), vol. 284, no. 1, p. 285-299 **284**, 285 (1994).

[50] Y. P. Jing and Y. Suto, Density profiles of dark matter halo are not universal, Astrophys. J. Lett. **529**, L69 (2000), arXiv:astro-ph/9909478.

[51] P. S. Behroozi, R. H. Wechsler, and C. Conroy, The Average Star Formation Histories of Galaxies in Dark Matter Halos from z =0-8, Astrophys. J. **770**, 57 (2013), arXiv:1207.6105 [astro-ph.CO].